Journal of Superconductivity and Novel Magnetism (2019) 32:763–768
https://doi.org/10.1007/s10948-018-4771-z

ORIGINAL PAPER

Structural Characterization and Magnetic Properties of $SrCo_2Fe_{16}O_{27}$ Hexaferrite Synthesized by Citric Acid Sol-Gel Method

M. M. Yang[1] · X. Zhang[1,2] · Z. K. Zhao[1] · S. W. Wang[1,2] · X. Zhou[1] · Y. Bai[1] · Y. P. Shao[1] · R. Yao[1]

Received: 10 April 2018 / Accepted: 4 June 2018 / Published online: 14 June 2018

Abstract

The W-type $SrCo_2Fe_{16}O_{27}$ (SCFO) hexagonal ferrite samples were prepared by the sol-gel method using metal nitrate as raw material, citric acid as complexing agent, and water as solvent. The effects of different sintering temperatures and holding times on the phase composition and morphology properties were explored in detail by using the X-ray diffractometer and field emission scanning electron microscope. The X-ray diffraction, microstructure, and magnetic performance of most optimum sintering temperature and holding time of preparing single-phase SCFO hexagonal ferrite were investigated. The experimental results indicate that the best optimum sintering temperature and holding time of SCFO hexagonal ferrite are 1280 °C and 4 h, respectively. Field emission scanning electron microscopy results indicate that the size of the particles is about 5–10 μm. The result of magnetic measurement shows that SCFO hexagonal ferrite exhibits the soft magnetic property and the Curie temperature (T_C) is ~ 850 K. Furthermore, by analyzing the Arrott plot, the phase transition near the T_C is a secondary phase transition.

Keywords SCFO hexagonal ferrite · X-ray diffraction · Citric acid sol-gel method · Magnetic properties

1 Introduction

The term ferrites are used to refer to iron oxide and other ingredients. They have room-temperature ferromagnetic and insulating properties [1]. Hexagonal ferrites have the characteristics of chemical stability, high resistivity, high coercivity, abundant raw material sources, and low price, which are used in high-density magnetic recording media, microwave, satellite communications devices, and different electromagnetic devices operating in the radio-frequency region [2]. There are six kinds of fundamental types for hexagonal ferrite family: M, W, X, Y, Z, and U [3]. It has been reported that the abovementioned hexagonal ferrites with planar magneto-crystalline anisotropy possess the good magnetic efficiency and performance, compared with spinel ferrites [4, 5], which can be used as hard ferrite magnets, electromagnetic wave absorbers, magnetic recording media, and microwave devices.

The unit cell of the W-type hexagonal ferrite consists of the RS2R*S*2 stacking sequence, where R* and S* are represented by R and S rotated by 180° around the c-axis [6]. Based on the previous studies, the compositions and the crystal structure have an important influence on the performance of W-type hexagonal ferrite. Recently, lots of studies have been done to affect the magnetic properties by replacing the divalent cations without altering the iron content [7–9]. In this study, the W-type SCFO hexagonal ferrite is chosen as the main research object for further investigation.

As we known, the classical method for Sr ferrite ceramic preparation involves traditional metallurgical method [10], chemical coprecipitation method [11], standard ceramic [12], and sol-gel method [13]. Among these techniques, citric acid sol-gel method has the advantages of raw material molecular mixing, low reaction temperature, and easy control of ion substitution, which is an ideal choice for preparing W-type ferrite.

✉ X. Zhang
xzhang80@163.com

✉ S. W. Wang
swwang666@sohu.com

1 School of Materials Science and Engineering, Guilin University of Electronic Technology, Guilin 541004, China

2 Guangxi Key Laboratory of Information Materials, Guilin University of Electronic Technology, Guilin 541004, China

In this paper, we report the results of a systematic variation of the different sintering temperatures and holding times in SCFO hexagonal ferrite synthesized by the sol-gel method. Moreover, the temperature dependence of magnetization (M-T) as well as the magnetic transition points are discussed in our study, which are rarely studied. The value of saturation magnetization (M_s) at 300 K is about 75 emu/g, which is higher than the previous research results. Furthermore, we also have innovatively studied the type of magnetic conversion of W-type hexaferrites.

2 Experiment

In this study, the samples of SCFO were prepared using a citric acid sol-gel method. The stoichiometric amounts of powder of iron nitrate ($(Fe(NO_3)_2)\cdot 9H_2O$, AR grade), strontium nitrate ($Sr(NO_3)_2$, AR grade), and calcium nitrate ($(Co(NO_3)_2)\cdot 6H_2O$, AR grade) were dissolved in distilled water as a mixture. The molar ratios of Sr:Co:Fe was 1:2:16. Then, an appropriate amount of citric acid solution was added into the above mixture. Solution was heated at 80 °C for about 3 h, and a viscous gel was obtained. After that, it was freeze-dried in a chamber with dehydration reaction. After the self-propagating reaction, a brown-colored fluffy powder (called precursor powder) was obtained. The precursor powder was pressed in a stainless-steel die under a pressure of 20 MPa with 8 wt% polyvinyl alcohol as binder lubricant. The pressed toroidal samples were sintered in the temperature range of 1190–1350 °C for 2 h in air to get W-type hexagonal phase.

The X-ray diffraction (XRD) patterns were recorded at room temperature using an Empy-rean variable temperature X-ray diffractometer (Holland PANalytical BV Company) with Cu Kα (1.54056 Å) radiation and a graphite monochromator operated at 45 KV and 40 mA. The morphology and the grain size of the sample were measured by the US Company FEI Quanta 450 FEG field emission scanning electron microscope (FESEM), and the available energy-dispersive X-ray spectroscopy (EDX) equipment was used to chemical element analysis of the samples. The magnetic measurements were carried out with Physical Properties Measurement System (PPMS-9 T).

3 Results and Discussion

3.1 XRD Analysis

Figure 1a shows XRD patterns of the samples sintered at various temperatures when the holding time is 2 h. At 1190 °C, the M-type ferrite had formed along with the spinel ferrite $CoFe_2O_4$. With the sintering temperature rising to 1250 °C, the XRD result revealed that the sample had transformed into W-type phase, and there was no further change in phase up to 1300 °C. However, the peak intensity of XRD pattern is higher for 1280 °C. Figure 1b shows XRD patterns of the samples sintered at various holding times for 1280 °C. When the holding time is more than 4 h, a small amount of secondary phase has been determined. The XRD patterns show that the diffraction peaks of 1280 °C for 4 h match well with the standard patterns of the SCFO (ICDD PDF no. 00-054-0106, space group $P6_3/mmc$) and are chosen as the main performance researched object.

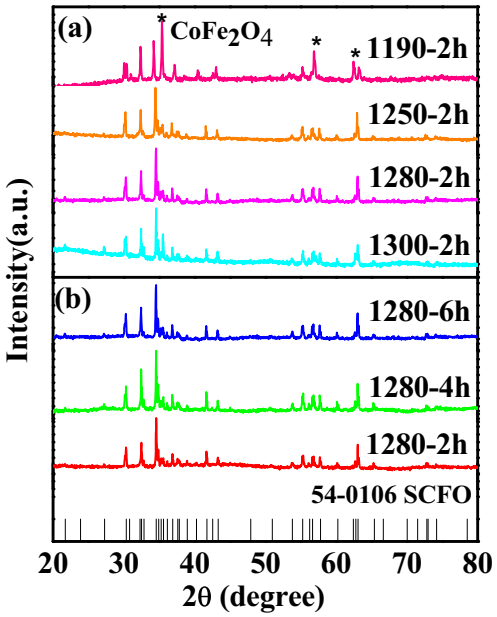

Fig. 1 **a** XRD patterns of SCFO hexaferrites for 1190–1300 °C with a holding time of 2 h. **b** XRD of SCFO with different holding times at 1280 °C

Figure 2 shows the powder XRD patterns and Rietveld refinement of the SCFO. As can be seen, all peaks can

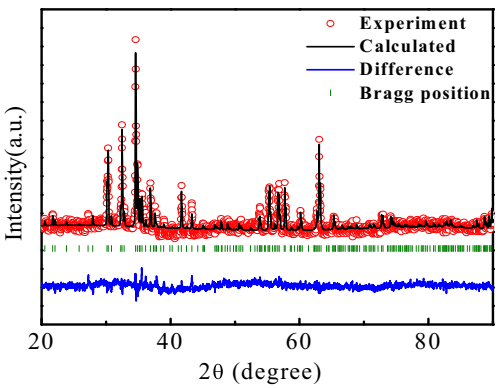

Fig. 2 X-ray powder diffraction pattern for the SCFO sample. Observed (circle), calculated (continuous line), and difference (bottom line) profiles at room temperature

Table 1 Structural parameters obtained from the Rietveld refinement of XRD pattern of SCFO with the space group $P6_3$/mm

Atom	Type	*X*	*Y*	*Z*
Sr1	Sr	0.0	0.0	0.2500
Fe1	Fe	0.3333	0.6667	− 0.2500
Fe2	Fe	0.3333	0.6667	− 0.4249(± 0.001)
Co1	Co	0.3333	0.6667	− 0.4249(± 0.001)
Fe3	Fe	0.5000	0.0	0.0
Co2	Co	0.5000	0.0	0.0
Fe4	Fe	0.0	0.0	0.0562(8)
Co3	Co	0.0	0.0	0.0562(± 0.0008)
Fe5	Fe	0.3333	0.6667	0.0951(± 0.0007)
Co4	Co	0.3333	0.6667	0.0951(± 0.0007)
Fe6	Fe	0.3333	0.6667	0.2045(± 0.0008)
Fe7	Fe	− 0.1643	− 0.3286	0.1506
O1	O	0.0	0.0	0.1085(± 0.0018)
O2	O	0.3333	0.6667	0.0306(± 0.0016)
O3	O	0.3333	0.6667	− 0.3085(± 0.0018)
O4	O	0.4880	0.9760	0.2500
O5	O	0.5037(± 0.0003)	1.0030(± 0.001)	0.1093(± 0.0014)
O6	O	− 0.1760	− 0.3520	0.03052
O7	O	0.1700	0.3400	0.1859(± 0.0011)

Lattice parameters (Å): $a = b = 5.891(\pm 0.003)$ and $c = 32.728(\pm 0.002)$. Bragg R factor = 19.2. $\chi^2 = 1.94$

be indexed by a hexagonal structure with the space group $P6_3$/mm. The FullProf least squares (Rietveld) technique results of the crystal structure are presented in Fig. 1 with the goodness-of-fitting $\chi^2 = 1.94$ and the lattice parameters of $a = b = 5.891(\pm 0.003)$ Å, $c = 32.728(\pm 0.002)$ Å, and $V = 983.7(\pm 0.1)$ Å^3, respectively. The details of structural parameters are listed in Table 1.

3.2 SEM Analysis

Figure 3 shows the SEM images of SCFO powders at different temperatures. It can be seen that most of the particles are hexagonal in shape. The size of the particles varies, ranging from 5 to 10 μm. As the temperature increases, the hexagonal morphology is gradually formed. When the temperature is up to 1280 °C and the holding time is 4 h, a good and uniform hexagonal platelet-like shape is formed with a random grain orientation. EDX spectra were collected from the cover of sample, as shown in Fig. 3e. The EDS pattern demonstrates the presence of Sr, Co, Fe, and O elements in the as-prepared sample. The average atomic mass of the sample was calculated several times to determine the stoichiometric ratio. Analysis of EDX spectra of the sample revealed that Fe:Sr = 17.5 ± 1.5, Co:Sr = 2.4 ± 0.4, and O:Sr = 25 ± 2. The overlapping between Fe-Kβ and Co-Kα spectral lines leads to a deviation of the spectral lines of Fe and Co. The results show that the molar ratio of Sr, Co, Fe, and O elements is 1:2.4:17.5:25. Combined with the result of XRD and SEM, we can draw the conclusion that the sample is single phase and close to the molar ratio of $SrCo_2Fe_{16}O_{27}$.

3.3 Magnetization Measurements

To understand the magnetic properties of SCFO, the low-field high-temperature M-T, the hysteresis loops, and the Arrott plot were investigated.

Figure 4 shows the magnetization as a function of temperature in the range 300–900 K in a magnetic field of 0.05 T. There are two drops at about 550 and 850 K. Few experimental results about the magnetization as a function of temperature was reported. Considering the similar results such as Z-type hexaferrites [14], we speculate that the two anomalies are likely to correspond to a transition from the phase with a cone of easy magnetization into the ferrimagnetic phase and a transition into a paramagnetic phase, respectively. The Curie temperature (T_C) is ~ 850 K.

Figure 5 shows the magnetic hysteresis (M-H) loops for the sample at several temperatures below T_C. The S-shaped loops of the SCFO hexaferrite show the typical soft character of magnets. In addition, the M_s of the sample increases with decreasing temperature. As seen in Fig. 5, the magnetization increases in two steps up to the saturation magnetization. In the first stage, the

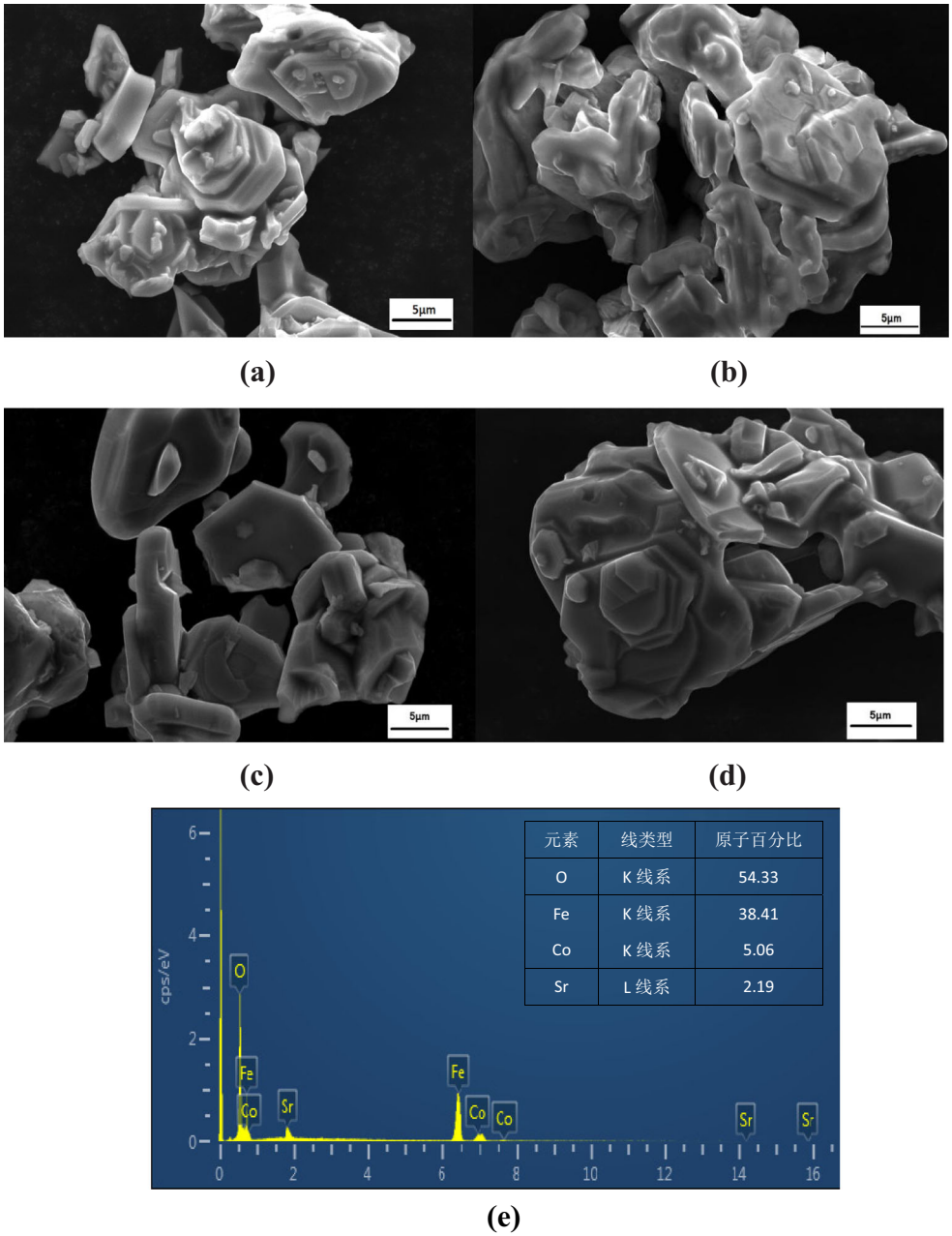

Fig. 3 SEM images for the SCFO hexaferrites of 1190 °C for 2 h, 1250 °C for 2 h, 1280 °C for 2 h, and 1280 °C for 4 h (**a**–**d**) and EDS spectra images (**e**)

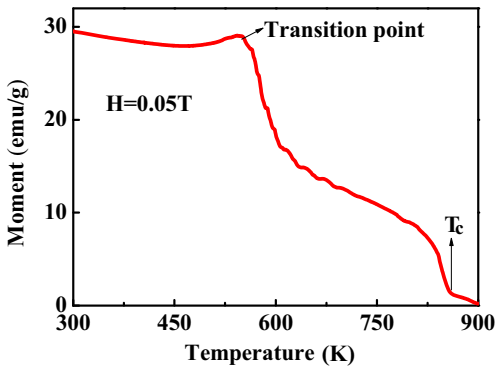

Fig. 4 Temperature dependence of the magnetization of SCFO in a field of 0.05 T

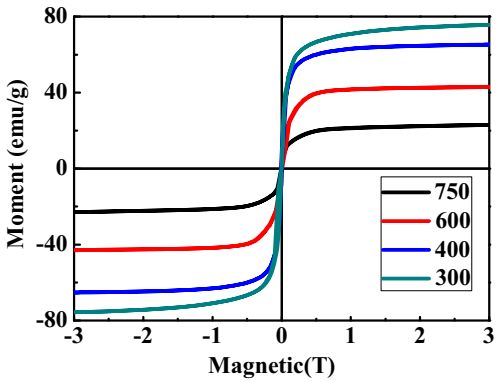

Fig. 5 The magnetic hysteresis loop of SCFO

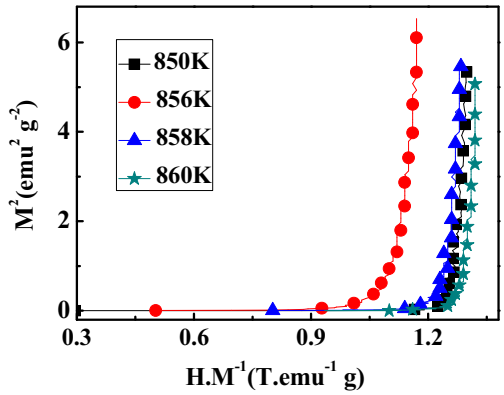

Fig. 6 The plots of HM^{-1} versus M^2 for SCFO at some selected temperatures

magnetization increases rapidly, while in the second stage, with the field increasing, the magnetization is changed slowly. The magnetic abnormity may be originated from the change of the magnetic structure [14]. The M_s is ~75.7 emu/g at 300 K, which is higher than the previous research results [15–17], while the coercive field (H_c) is comparatively low, suggesting that the sample exhibits strong magnetism and expands its application area.

Figure 6 shows the Arrott curve of the sample. As we know, in the framework of the Landau phase transition theory, the magnetization and magnetic field near T_C satisfy $A+ BM^2 = u_0HM^{-1}$, where A and B are the Landau coefficients. The magnetic transition is a second order if all the HM^{-1} versus M^2 curves only have positive slope, while if the HM^{-1} versus M^2 curves show both positive and negative slopes, the magnetic transition is the first order. As shown in Fig. 6, the slope near T_C is positive and there is no change from positive to negative, indicating that the phase transition is a secondary phase transition.

4 Conclusions

Single-phase SCFO hexaferrites have been successfully synthesized by a sol-gel method at the optimum preparation conditions. The preburning temperature and calcination temperature are 600 and 1280 °C, respectively. SEM results indicate that the size of the particles is about 5–10 μm. Structure analysis reveals that our samples crystallize in the hexagonal structure with the space group $P6_3/mmc$.

According to the high-temperature M-T curve, the sample exhibits two phase transition points (~550 and 850 K). They are likely to correspond to a transition from the phase with a cone of easy magnetization into the ferrimagnetic phase and a transition into a paramagnetic phase, respectively. The hysteresis loops of SCFO ferrite exhibit soft magnetic properties, and the magnetization increases in two steps up to the saturation magnetization, which may originate from the change of the magnetic structure. The Arrott curve shows that the phase transition near T_C is a secondary phase transition.

Funding Information This work was supported by the National Science Foundation of China (Grant No. 11464007), the National Science Foundation of Guangxi (Grant No. 2017GXNSFAA198373), the Guangxi Key Laboratory of Information Material Foundation (Grant Nos. 171020-Z and 171025-Z), and the Graduate Student Innovation Project of Guilin University of Electronic Technology (Grant No. 2017YJCXB01).

References

1. Sugimoto, M.: Am. J. Ceram. Soc. **82**, 269–280 (1999)
2. Nakamura, T., Hatakeyama, K.: Complex permeability of polycrystalline hexagonal ferrites. IEEE. Trans. Magn. **36**, 3415–3417 (2000)
3. Ghasemi, A.: Effects of divalent ion substitution on the microstructure and magnetic properties of $SrCo_{2-x}(MnZnCa)_{x/3}Fe_{16}O_{27}$, nanoparticles. J. Supercond. Nov. Magn. **29**, 1943–1952 (2016)
4. Smit, J., Wijin, H.P.: Ferrites, p. 185. Cleaver-Hume, London (1959)
5. Ahmad, M., Grössinger, R., Kriegisch, M., Kubel, F., Rana, M.: Magnetic and microwave attenuation behavior of Al-substituted Co_2W hexaferrites synthesized by sol-gel auto-combustion process. J. Curr. Appl. Phys. **12**, 1413–1420 (2012)
6. Mahmood, S.H., Aloqaily, A.N., Maswadeh, Y., Ahmad, A., Ibrahim, B., Mufeed, A., Hassan, J.: Effects of heat treatment on the phase evolution, structural, and magnetic properties of Mo-Zn doped M-type hexaferrites. J. Solid State Phenomena **232**, 65–92 (2015)
7. Rai, G.M., Aen, F., Islam, M.U., Rana, M.: Dielectric and magnetic behavior of $BaCd_{2-x}Sr_xFe_{16}O_{27}$ W-type hexagonal ferrites. J. Alloy Compd. **509**, 4793–4796 (2011)
8. Kimura, T.: Magnetoelectric hexaferrites. J. Annu. Rev. Condens. Matter. Phys. **3**, 93–110 (2012)
9. Huang, X., Zhang, J., Wang, H., Yan, S., Wang, L., Zhang, Q.: Er-substituted W-type barium ferrite: preparation and electromagnetic properties. J. Rare. Earth **28**, 940–943 (2010)
10. Tung, M.J., Chen, R., Hsu, C.H., Tseng, T.Y.: A model of non-homogeneous damped electromagnetic wave and heat equation in ferrite materials. J. Magn. Magn. Mater. **239**, 402–405 (2002)
11. Wang, J., Zhang, H., Bai, S.X., Chen, K., Zhang, C.: Microwave absorbing properties of rare-earth elements substituted W-type barium ferrite. J. Magn. Magn. Mater. **312**, 310–313 (2007)
12. Ahmed, M.A., Okasha, N., Oaf, M., Kershi, R.M.: The role of Mg substitution on the microstructure and magnetic properties of BaCoZn W-type hexagonal ferrites. J. Magn. Magn. Mater. **314**, 128–134 (2007)
13. Qiu, J., Liang, L., Gu, M.: Nanocrystalline structure and magnetic properties of barium ferrite particles prepared via glycine as a fuel. J. Mater. Sci. Eng. R **393**, 361–365 (2005)
14. Yutaro, K., Yuji, H., Takashi, H., Taishi, I., Hiroyuki, N., Tsuyoshi, K.: Low-field magnetoelectric effect at room temperature. J. Nat. Mater. **9**(10), 797 (2010)
15. Niu, X., Liu, Y., Li, M., Wu, B., Li, H.: The study of microstructure and magnetic properties of La^{3+} doped W-type hexagonal ferrites $Sr_{1-x}La_xCo_2Fe_{16}O_{27}$. J. Electron. Mater. **46**, 4299–4303 (2017)

16. Ali, A., Grössinger, R., Imran, M., Khan, M.A., Elahi, A., Akhtar, M.N., Mustafa, G., Khan, M.A., Ullah, H., Murtaza, G., Ahmad, M.: Magnetic and high-frequency dielectric parameters of divalent ion-substituted W-type hexagonal ferrites. J. Electron. Mater. **46**, 1–8 (2017)

17. Ahmad, M., Grössinger, R., Kriegisch, M., Kubelc, M.F., Ranaa, U.: Characterization of Sr-substituted W-type hexagonal ferrites synthesized by sol–gel autocombustion method. J. Magn. Magn. Mater. **332**(4), 137–145 (2013)